Supporting Information

Ciani et al. 10.1073/pnas.1008502107

SI Methods.

Peptide Preparations. Construction, recombinant expression in bacteria, and purification of all the GCN4-p1 variants were performed as described (1). The Cort-Ir variants were prepared by PCR amplification of the entire pET15b-Ir plasmid (2) using oligonucleotide primers that encode the mutated regions. For DNA recircularization and repair, the PCR products were transfected into the MACH1 (Invitrogen) *Escherichia coli* strain. Bacterial expression and purification were performed as described previously (2). Human ATF1-p and its variants were expressed from synthetic genes with optimal codon useage for *E. coli*. The peptides were purified as described (1). GCN4-p1 and ATF1-p peptides contain two (GlySer) and Cort-Ir polypeptide chain fragments harbor four additional residues (HisMetGlySer) at their N termini, which originate from recombinant expression. Peptide stock solutions were prepared in 5 mM sodium phosphate, pH 7.4 supplemented with 150 mM PBS (for solution studies). Concentrations of peptide samples were determined by tyrosine absorption at 280 nm.

Crystal Structure Determination. Crystals of GCN4-pM3 and GCN4-pM7 were grown at 20 °C by mixing equal volumes of proteins (5–15 mg/mL) with reservoir solutions by using the sitting drop method. Crystals grew within 1 d using reservoir solutions containing 0.2 M sodium citrate, 0.1 M sodium cacodylate (pH 6.5), 30% 2-propanol (GCN4-pM3) or 0.1 M Tris-HCl (pH 8.5), 30% (vol/vol) PEG 400 (GCN4-pM7).

Datasets were collected at 100 K by using CuKα radiation produced by a rotating anode generator. Data collection and refinement statistics are given in Table S1. The structures were solved by molecular replacement by using a three-stranded GCN4-p1 variant (PDB ID code 1ZIJ) as a search model. Figures were prepared with PyMOL (DeLano Scientific LLC, www.pymol.org).

1. Harbury PB, Kim PS, Alber T (1994) Crystal structure of an isoleucine-zipper trimer. *Nature* 371:80–83.
2. Frank S, Lustig A, Schulthess T, Engel J, Kammerer RA (2000) A distinct seven-residue trigger sequence is indispensable for proper coiled-coil formation of the human macrophage scavenger receptor oligomerization domain. *J Biol Chem* 275:11672–11677.

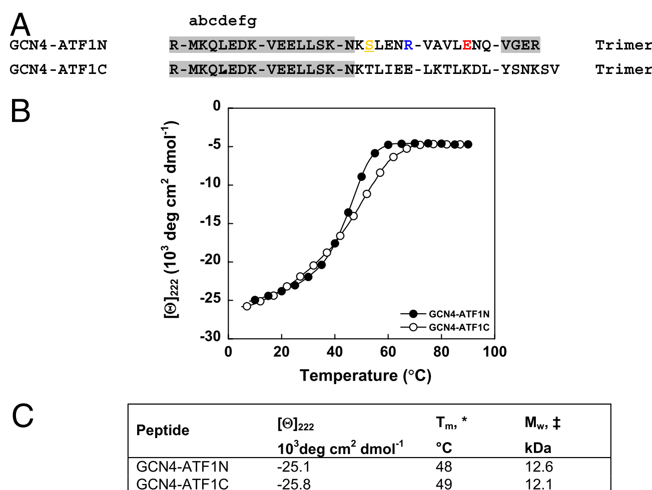

Peptide	$[\Theta]_{222}$ 10^3deg cm^2 dmol^{-1}	T_m, * °C	M_w, ‡ kDa
GCN4-ATF1N	-25.1	48	12.6
GCN4-ATF1C	-25.8	49	12.1

Fig. S1. Characterization of GCN4-ATF1 chimeras. (*A*) Rational design. Details regarding heptad-repeat pattern and color coding of residues are described in Fig. 1*A*. The sequences originating from GCN4-p1 are highlighted in gray. The oligomerization state of the peptides is indicated on the right. (*B*) CD analysis. Thermal unfolding profiles recorded by CD at 222 nm of GCN4-ATF1N and GCN4-ATF1C are shown. The experiments were carried out at 35-μM peptide concentration (monomer) in PBS (pH 7.4). (*C*) CD, sedimentation equilibrium analytical ultracentrifugation (AUC), and multiangle light scattering data. *, T_m determined at peptide concentrations (monomer) of 35 μM; ‡, average molecular masses determined by AUC. The calculated molecular masses of GCN4-ATF1N and GCN4-ATF1C are 4.0 kDa and 4.2 kDa, respectively.

Fig. S2. CD analysis of Cort-Ir variants. Thermal unfolding profiles recorded by CD at 222 nm of Cort-Ir, Cort-Ir-M1, Cort-Ir-M2, Cort-Ir-M3, Cort-Ir-M4, and Cort-Ir-M6 are shown. The experiments were carried out at 35-μM peptide concentration (monomer) in PBS (pH 7.4).

Fig. S3. Analysis of the oligomerization state of Cort-Ir variants by sedimentation equilibrium analysis. The sequences of Cort-Ir-M6 and Cort-Ir-M8 are shown in Fig. 1*C*. (*Upper*) UV absorbance gradients as a function of radial position (data points) and fits according to a single ideal species model (red lines). (*Lower*) Residuals showing the difference between the experimental data and the theoretical model. The fitted values are listed in Table 1. The sedimentation profiles were monitored at two wavelengths (275 nm for tyrosine and 235 nm for peptide backbone absorption) and three different speeds. All data were fitted simultaneously.

A B

Fig. S4. X-ray crystal structures of the (*A*) GCN4-pM3 and (*B*) GCN4-pM7 trimers. Side views with the N terminus on top. Side chains and backbones are shown as sticks and cartoon representation, respectively. Oxygen and nitrogen atoms are colored in red and blue, and carbon atoms are shown in green, cyan, and yellow for monomers A, B, and C, respectively. Residues Arg22 to Glu27 that form the trimerization motif and introduced isoleucine residues are shown as van der Waals spheres. For the sequences of the GCN4-p1 variants, see Fig. 1*A*.

Table S1. Data collection and refinement statistics

	GCN4-pM3	GCN4-pM7
Wavelength, Å	1.54	1.51
Space group	C2	P212121
Resolution, Å	1.86	2.0
Unit cell, *a*, *b*, and *c* in Å; α, β, and γ in °	76.1, 56.3, 54.9; 90.0, 129.0, 90.0	42.2, 45.9, 47.1; 90.0, 90.0, 90.0
No. of observed reflections	56,071 (10,488)*	17,572 (2,348) *
No. of unique reflections	15,146 (2,915)*	6,442 (863)*
R_{sym}, %[†]	3.8 (16.2)*	4.9 (12.9)*
$I/\sigma(I)$	22.4 (7.6)*	15.7(7.6)*
Completeness, %	98.8 (98.2)*	98.1(98.6)*
No. of refined atoms		
Proteins	1596	861
Water	189	63
R-factor/free *R*-factor[‡]	0.18/0.23	0.22/0.26
rmsd bond lengths/bond angles[§]	0.01/1.1	0.01/1.1

*Figures in parentheses indicate the values for the outer shell of the data.

[†] $R_{sym} = \sum_h \sum_i |I_i(h) - \langle I(h) \rangle| / \sum_h \sum_i I_i(h)$, where $I_i(h)$ and $\langle I(h) \rangle$ are the *i*th and mean measurement of the intensity of reflection *h*.

[‡] $R = \sum |F_P{}^{obs} - F_P{}^{calc}| / \sum F_P{}^{obs}$, where $F_P{}^{obs}$ and $F_P{}^{calc}$ are the observed and calculated structure factor amplitudes, respectively.

[§] rmsd, root-mean-square deviation from the parameter set for ideal stereochemistry.